Mathematics Today Vol.34(A) (April 2018 – Special Issue) 7-24
ISSN 0976-3228, e-ISSN 2455-9601

Mathematical Analysis of three dimensional nanofluid flow in a rotating system considering thermal interfacial resistance and Brownian motion in suspensions through porous medium

Dr. Hari R. Kataria[1], Mr. Akhil S. Mittal [2]

[1]Department of Mathematics, Faculty of Science,
The M. S. University of Baroda, Vadodara, India
[1]hrkrmaths@yahoo.com

[2] Department of Mathematics,
Gujarat Science College, Ahmedabad, India
[2]akhilsmittal@gmail.com

Corresponding author: Mr. Akhil S. Mittal [2]
[2] Department of Mathematics,
Gujarat Science College, Ahmedabad, India
[2]akhilsmittal@gmail.com

[2]Phone Number: 91-9228340320

Abstract

In the present investigation, three dimensional MHD nanofluid flow between two horizontal parallel plates through porous medium in rotating system is scrutinized. Effects of thermal interfacial resistance, nanoparticle volume fraction, Brownian motion and nanoparticle size on thermal conductivity are considered. Also micro mixing in suspensions is taken into account while calculating viscosity. Homotopy Analysis method is employed to solve the system of ordinary differential equations, obtained by reducing original system of partial differential equations using suitable change of variables. Effects of different prevailing parameters on Heat transfer and fluid flow are discussed. Also it is observed that the skin friction increases with increase in rotation parameter but decreases when nanoparticle volume fraction increases. The magnitude of Nusselt number rises with Reynolds number and nanoparticle volume fraction but it declines with increase of rotation parameters and Eckert number.

Keywords: HAM; MHD; Nanofluid; Brownian; Heat transfer;
AMS Subject Classification: 76W05, 76W99

Nomenclature

T	Temperature
T_w	Temperature
u, v, w	Velocity components along x, y, z axes, respectively
B	External uniform magnetic field

C_p Specific heat at constant pressure

g Acceleration due to gravity

k Thermal conductivity

k_1 Permeability of the fluid

M Magnetic parameter (Ratio of Lorentz force to viscous force)

Pr Prandtl number (ratio of momentum diffusivity to thermal diffusivity)

Greek symbols

α Thermal diffusivity

ρ Density

σ Electrical conductivity (S/m)

$\emptyset$ Nanoparticle volume fraction

θ Dimensionless temperature ($\theta = \frac{T-T_0}{T_w-T_0}$)

μ Dynamic viscosity

φ Porosity

κ Permeability (dimensionless)

Ω Constant Rotation velocity

ν Kinematic viscosity

η Dimensionless variable

Subscripts

f Fluid phase

nf Nano-fluid

s Solid phase

1. Introduction

Effect of magnetic field on electrically conducting fluids has applications in engineering and reak world problems such as generators, coolant in huge nuclear power plants, plasma and bearings. Kataria and Mittal [1] modelled gravity-driven convective optically thick nanofluid flow past an oscillating vertical plate. This work was extended considering mass transfer by Kataria and Mittal [2]. Kataria and Mittal [3] investigated effect of radiation on Casson nanofluid flow. Kataria and Patel [4] discussed effects of thermo-diffusion and parabolic motion on Second grade fluid flow. Casson fluid flow was studied by Kataria and Patel [5-6]. Kataria and Patel [7] discussed effect of magnetic field on unsteady micropolar fluid flow between two vertical walls. Kataria and Patel [8] studied heat and mass transfer in second grade fluid flow. Effect of radiation on nanofluid flow was illustrated by Sheikholeslami et al. [12].

This study is carried out to extend the study of nanofluid flow to three dimension in presence of magnetic field and thermal radiation between horizontal parallel plates in a rotating system. Effects of many vital phenomenon

like Brownian motion, thermal interfacial resistance, nanoparticle volume fraction, nanoparticle size and base fluid on thermal conductivity are taken into account.

The simplified system of ordinary differential equations are solved using the Homotopy analysis method. The effects of the pertinent parameters are discussed.

2. Problem statement and Mathematical Formulation:

Nanofluid under consideration is water based nanofluid containing Al_2O_3 nanoparticles. Flow is between two horizontal parallel plates, placed L units apart through a porous medium. A coordinate system (x, y, z) is chosen such that origin is positioned at the lower plate. Two forces of equal magnitude in opposite directions are applied on the lower plate. The plates along with the fluid rotate about y axis with angular velocity Ω. A uniform magnetic flux with density B is applied along y-axis. Under these assumptions, governing equations [13] are:

$$\frac{\partial u}{\partial x}+\frac{\partial v}{\partial y}+\frac{\partial w}{\partial z}=0 \tag{1}$$

$$\rho_{nf}\left(u\frac{\partial u}{\partial x}+v\frac{\partial u}{\partial y}+2\Omega w\right)=\mu_{nf}\left(\frac{\partial^2 u}{\partial x^2}+\frac{\partial^2 u}{\partial y^2}\right)-\sigma_{nf}B^2u-\frac{\mu_{nf}\varphi}{k_1}u \tag{2}$$

$$\rho_{nf}\left(v\frac{\partial v}{\partial y}\right)=\mu_{nf}\left(\frac{\partial^2 v}{\partial x^2}+\frac{\partial^2 v}{\partial y^2}\right) \tag{3}$$

$$\rho_{nf}\left(u\frac{\partial w}{\partial x}+v\frac{\partial w}{\partial y}-2\Omega w\right)=\mu_{nf}\left(\frac{\partial^2 w}{\partial x^2}+\frac{\partial^2 w}{\partial y^2}\right)-\sigma_{nf}B^2w-\frac{\mu_{nf}\varphi}{k_1}w \tag{4}$$

$$\left(\rho c_p\right)_{nf}\left(u\frac{\partial T}{\partial x}+v\frac{\partial T}{\partial y}+w\frac{\partial T}{\partial z}\right)=k_{nf}\left(\frac{\partial^2 T}{\partial x^2}+\frac{\partial^2 T}{\partial y^2}+\frac{\partial^2 T}{\partial z^2}\right)+$$
$$\mu_{nf}\left(2\left[\left(\frac{\partial u}{\partial x}\right)^2+\left(\frac{\partial v}{\partial y}\right)^2+\left(\frac{\partial w}{\partial z}\right)^2\right]+\left(\frac{\partial v}{\partial x}\right)^2+\left(\frac{\partial v}{\partial z}\right)^2+\left(\frac{\partial w}{\partial x}+\frac{\partial u}{\partial z}\right)^2\right) \tag{5}$$

where

$$\rho_{nf}=(1-\emptyset)\rho_f+\emptyset\rho_s \tag{6}$$

$$\sigma_{nf}=\sigma_f[1+\frac{3(\sigma-1)\emptyset}{(\sigma+2)-(\sigma-1)\emptyset}],\ \sigma=\frac{\sigma_s}{\sigma_f} \tag{7}$$

$$\left(\rho c_p\right)_{nf}=(1-\emptyset)(\rho c_p)_f+\emptyset(\rho c_p)_s \tag{8}$$

Effects of thermal interfacial resistance, nanoparticle volume fraction, Brownian motion, nanoparticle size, types of nanoparticle and base fluid on thermal conductivity [9] are considered. Also micro mixing in suspensions is taken into account while calculating viscosity.

$$k_{eff}=k_{static}+k_{Brownian}=k_f\left[1-3\frac{\emptyset(k_f-k_{s,R})}{2k_f+k_{s,R}+\emptyset(k_f-k_{s,R})}\right]+5\times10^4\emptyset\rho_f c_{pf}\sqrt{\frac{\kappa_b T}{\rho_s d_s}}F(T,\emptyset,d_s), \tag{9}$$

$$k_{s,R}=\frac{k_s d_s}{R_f k_s+d_s} \tag{10}$$

$$F(T,\emptyset,d_s)=\left(A_1+A_2\ln(d_s)+A_3\ln(\emptyset)+A_4\ln(\emptyset)\ln(d_s)+A_5\ln\left(d_s{}^2\right)\right)\ln(T)+\left(A_6+A_7\ln(d_s)+\right.$$
$$\left.A_8\ln(\emptyset)+A_9\ln(\emptyset)\ln(d_s)+A_{10}\ln\left(d_s{}^2\right)\right) \tag{11}$$

With

$R_f=4*10^{-8}Km^2/W$ is thermal interfacial resistance. (12)

$$A_1 = 52.813488759, \quad A_2 = 6.115637295, \quad A_3 = 0.6955745084, \quad A_4 = .0417455552786,$$
$$A_5 = 0.176919300241, \; A_6 = -298.19819084, A_7 = -34.532716906, \; A_8 = -3.9225289283,$$
$$A_9 = -0.2354329626, \; A_{10} = -0.999063481 \tag{13}$$

(Here it must be noted that these values are not general and vary with nanofuid, the nanofluid in this article is Al_2O_3-Water nanofluid.)

Considering effect of "micro mixing in suspensions" on viscosity [10], we get

$$\mu_{nf} = \mu_{static} + \mu_{Brownian} = \frac{\mu_f}{(1-\emptyset)^{2.5}} + \frac{k_{Brownian} * \mu_f}{k_f * Pr_f} \tag{14}$$

The thermo-physical properties of water and nanoparticles are as in Table 1 [9].

Subject to

$$u = ax; \; v = 0; \; w = 0; \; T = T_w \; at \; y = 0 \tag{15}$$

$$u = 0; \; v = 0; \; w = 0; \; T = T_L \; at \; y = L \tag{16}$$

Introducing non dimensional variables

$$\eta = \frac{y}{L}, \; u = axf'(\eta), v = -ahf(\eta), \; w = axg(\eta), \; \theta(\eta) = \frac{T - T_L}{T_w - T_L} \tag{17}$$

Therefore, the governing momentum and energy equations for this problem are given in dimensionless form by:

$$a_1 f^{iv} - Re(f'f'' - ff''') - 2Krg' - \left(a_3 M^2 + \frac{a_1}{k}\right) f'' = 0 \tag{18}$$

$$a_1 g'' - Re(f'g - fg') + 2Krf' - \left(a_3 M^2 + \frac{a_1}{k}\right) g = 0 \tag{19}$$

$$\theta'' + Pr\left(Rea_2 f\theta' + Eca_4(4f'^2 + g^2)\right) = 0 \tag{20}$$

where

$$Pr = \frac{\mu_f (c_p)_f}{k_f}, M^2 = \frac{\sigma_f {B_0}^2 L^2}{\rho_f v_f}, \; \frac{1}{\kappa} = \frac{v\varphi^2}{k_1 v_f}, \; Kr = \frac{\Omega L^2}{v_f}, Re = \frac{aL^2}{v_f}, Ec = \frac{(aL)^2}{(c_p)_f (\theta_0 - \theta_L)} \tag{21}$$

$$b_0 = 1 - \emptyset \tag{22}$$

$$b_1 = (b_0 + \emptyset \frac{\rho_s}{\rho_f}), \tag{23}$$

$$b_2 = \frac{1}{{b_0}^{2.5}} \tag{24}$$

$$b_3 = (b_0 + \emptyset \frac{(\rho c_p)_s}{(\rho c_p)_f}), \tag{25}$$

$$b_4 = \frac{k_{nf}}{k_f}, \tag{26}$$

$$b_5 = \frac{\sigma_{nf}}{\sigma_f}, \tag{27}$$

$$a_1 = \frac{1}{{b_0}^{2.5} b_1}, \tag{28}$$

$$a_2 = \frac{b_3}{b_4}, \tag{29}$$

$$a_3 = \frac{b_5}{b_1}, \tag{30}$$

$$a_4 = \frac{b_2}{b_4}, \tag{31}$$

Subject to

$$f = 0, f' = 1, g = 0, \theta = 1 \; at \; \eta = 0 \tag{32}$$

$$f = 0, f' = 0, g = 0, \theta = 0 \; at \; \eta = 1 \tag{33}$$

Table 1 Thermo-physical properties of the base fluid and nanoparticles [9].

Physical properties	Fluid phase (water)	Al_2O_3
$C_p(J/KgK)$	4179	765
$\rho(Kg/m^3)$	997.1	3970
$K(W/mK)$	0.613	25
$d_s(nm)$	----	47
$\sigma(\Omega m)^{-1}$	0.05	10^{-12}

3. Solution

Homotopy analysis method is a fundamental concept of topology. Equations (18) – (20) are coupled non-linear ordinary differential equations and exact solutions are not possible. To solve these equations together with the boundary conditions (33), the modified homotopy analysis method (HAM) suggested by Liao [11] is employed. Initial guess is given by:

$$f_0(\eta) = \frac{-2}{e^2-4e+3} + \frac{e-1}{e-3}\eta + \frac{2-e}{e^2-4e+3}e^{\eta} + \frac{e}{e^2-4e+3}e^{-\eta}; \;\; g_0(\eta) = 0; \;\; \theta_0(\eta) = 1 - \eta; \tag{34}$$

with auxiliary linear operators:

$$L_f = \frac{\partial^4 f}{\partial \eta^4} - \frac{\partial^2 f}{\partial \eta^2}, \;\; L_g = \frac{\partial^2 g}{\partial \eta^2} - \frac{\partial g}{\partial \eta}, \;\; L_\theta = \frac{\partial^2 \theta}{\partial \eta^2} \tag{35}$$

Satisfying

$$L_f(C_1 + C_2\,\eta + C_3 e^{\eta} + C_4 e^{-\eta}) = 0, \;\; L_g(C_5 + C_6 e^{\eta}) = 0, \;\; L_\theta(\,C_7 + C_8\eta) = 0. \tag{36}$$

where $c_1, \;\; c_2, \ldots., c_8$ are the arbitrary constants.

The zero[th] order deformation problems are constructed as follows:

$$(1-p)L_f\left[\hat{f}(\eta;\, p) - f_0(\eta)\right] = p\hbar_f N_f\left[\hat{f}(\eta;\, p), \hat{g}(\eta;\, p), \hat{\theta}(\eta;\, p)\right], \tag{37}$$

$$(1-p)L_g[\hat{g}(\eta;\, p) - g_0(\eta)] = p\hbar_g N_g\left[\hat{f}(\eta;\, p), \hat{g}(\eta;\, p), \hat{\theta}(\eta;\, p)\right], \tag{38}$$

$$(1-p)L_\theta\left[\hat{\theta}(\eta;\, p) - \theta_0(\eta)\right] = p\hbar_\theta N_\theta\left[\hat{f}(\eta;\, p), \hat{g}(\eta;\, p), \hat{\theta}(\eta;\, p)\right], \tag{39}$$

Subject to the boundary conditions:

$$\hat{f}(0;\, p) = 0, \quad \hat{f}'(0;\, p) = 1; \tag{40}$$

$$\hat{f}(1;\, p) = 0, \quad \hat{f}'(1;\, p) = 0; \tag{41}$$

$$\hat{g}(0;\, p) = 0, \quad \hat{g}(1;\, p) = 0; \tag{42}$$

$$\hat{\theta}(0;\, p) = 1, \quad \hat{\theta}(1;\, p) = 0, \tag{43}$$

The nonlinear operator are defined as

$$N_f\left[\hat{f}(\eta;\ p), \hat{g}(\eta;\ p), \hat{\theta}(\eta;\ p)\right] = a_1 \frac{\partial^4 \hat{f}}{\partial \eta^4} - Re\left(\frac{\partial \hat{f}}{\partial \eta}\frac{\partial^2 \hat{f}}{\partial \eta^2} - \hat{f}\frac{\partial^3 \hat{f}}{\partial \eta^3}\right) - 2Kr\ \frac{\partial \hat{g}}{\partial \eta} - \left(a_3 M^2 + \frac{a_1}{k}\right)\frac{\partial^2 \hat{f}}{\partial \eta^2}, \tag{44}$$

$$N_g\left[\hat{f}(\eta;\ p), \hat{g}(\eta;\ p), \hat{\theta}(\eta;\ p)\right] = a_1 \frac{\partial^2 \hat{g}}{\partial \eta^2} - Re\left(g\ \frac{\partial \hat{f}}{\partial \eta} - f\ \frac{\partial \hat{g}}{\partial \eta}\right) + 2Kr\ \frac{\partial \hat{f}}{\partial \eta} - \left(a_3 M^2 + \frac{a_1}{k}\right) g, \tag{45}$$

$$N_\theta\left[\hat{f}(\eta;\ p), \hat{g}(\eta;\ p), \hat{\theta}(\eta;\ p)\right] = \frac{\partial^2 \hat{\theta}}{\partial \eta^2} + Pr\left(Rea_2 \hat{f}\frac{\partial \hat{\theta}}{\partial \eta} + Eca_4\left(4\left(\frac{\partial \hat{f}}{\partial \eta}\right)^2 + g^2\right)\right) \tag{46}$$

Where $\hat{f}(\eta;\ p), \hat{g}(\eta;\ p)$ and $\widehat{\theta}(\eta;\ p)$ are unknown functions with respect to η and p. $\hbar_f$, $\hbar_g$ and $\hbar_\theta$ are the non-zero auxiliary parameters and N_f, N_g and N_θ are the nonlinear operators.

Also $p \in (0,\ 1)$ is an embedding parameter. For $p = 0$ and $p = 1$ we have

$$\hat{f}(\eta; 0) = f_0(\eta), \hat{f}(\eta; 1) = f(\eta), \tag{47}$$

$$\hat{g}(\eta; 0) = g_0(\eta), \hat{g}(\eta; 1) = g(\eta), \tag{48}$$

$$\hat{\theta}(\eta; 0) = \theta_0(\eta), \hat{\theta}(\eta; 1) = \theta(\eta), \tag{49}$$

In other words, when variation of p is taken from 0 to 1 then $\hat{f}(\eta;\ p)$, $\hat{g}(\eta;\ p)$ and $\hat{\theta}(\eta;\ p)$ vary from $f_0(\eta)$, $g_0(\eta)$, and $\theta_0(\eta)$ to $f(\eta), g(\eta),$ and $\theta(\eta)$. Taylor's series expansion of these functions yields the following:

$$\hat{f}(\eta;\ p) = f_0(\eta) + \sum_{m=1}^{\infty} f_m(\eta) p^m, \tag{50}$$

$$\hat{g}(\eta;\ p) = g_0(\eta) + \sum_{m=1}^{\infty} g_m(\eta) p^m, \tag{51}$$

$$\hat{\theta}(\eta;\ p) = \theta_0(\eta) + \sum_{m=1}^{\infty} \theta_m(\eta) p^m, \tag{52}$$

Where

$$f_m(\eta) = \frac{1}{m!}\left[\frac{\partial^m f(\eta; p)}{\partial p^m}\right]_{p=0}, \tag{53}$$

$$g_m(\eta) = \frac{1}{m!}\left[\frac{\partial^m g(\eta; p)}{\partial p^m}\right]_{p=0}, \tag{54}$$

$$\theta_m(\eta) = \frac{1}{m!}\left[\frac{\partial^m \theta(\eta; p)}{\partial p^m}\right]_{p=0}, \tag{55}$$

It should be noted that the convergence in the above series strongly depends upon $\hbar_f, \hbar_g$ and $\hbar_\theta$. Assuming that these nonzero auxiliary parameters are chosen so that Equations (35)-(37) converges at $p = 1$, Hence one can obtain the following:

$$f(\eta) = f_0(\eta) + \sum_{m=1}^{\infty} f_m(\eta), \tag{56}$$

$$g(\eta) = g_0(\eta) + \sum_{m=1}^{\infty} g_m(\eta), \tag{57}$$

$$\theta(\eta) = \theta_0(\eta) + \sum_{m=1}^{\infty} \theta_m(\eta), \tag{58}$$

Differentiating the zeroth order deformation (37) – (39) and (40) – (43) m times with respect to p and substituting $= 0$, and finally dividing by $m!$, we obtain the m[th] order deformation ($m \geq 1$).

$$L_f[f_m(\eta) - \chi_m f_{m-1}(\eta)] = \hbar_f R_{f,m}(\eta), \tag{59}$$

$$L_g[g_m(\eta) - \chi_m g_{m-1}(\eta)] = \hbar_g R_{g,m}(\eta), \tag{60}$$

$$L_\theta[\theta_m(\eta) - \chi_m \theta_{m-1}(\eta)] = \hbar_\theta R_{\theta,m}(\eta), \tag{61}$$

Subject to the boundary conditions

$$f_m(0) = f_m'(0) = 0, \tag{62}$$

$$f_m(1) = f_m'(1) = 0, \tag{63}$$

$$g_m(0) = g_m(1) = 0, \tag{64}$$

$$\theta_m(0) = \theta_m(1) = 0, \tag{65}$$

with

$$R_{f,m}(\eta) = a_1 f_{m-1}^{iv} - Re\left(\sum_{j=0}^{m-1} f_j' f_{m-1-j}'' - \sum_{j=0}^{m-1} f_j f_{m-1-j}'''\right) - 2Kr g_{m-1}' - \left(a_3 M^2 + \frac{a_1}{k}\right) f_{m-1}'' \tag{66}$$

$$R_{g,m}(\eta) = a_1 g_{m-1}'' - Re\left(\sum_{j=0}^{m-1} f_j'\, g_{m-1-j} - \sum_{j=0}^{m-1} f_j g_{m-1-j}'\right) + 2Kr f_{m-1}' - \left(a_3 M^2 + \frac{a_1}{k}\right) g_{m-1} \tag{67}$$

$$R_{\theta,m}(\eta) = \theta_{m-1}'' + Pr\left(Re a_2 \sum_{j=0}^{m-1} f_j \theta_{m-1-j}' + Ec a_4\left(4\sum_{j=0}^{m-1} f_j' f_{m-1-j}' + \sum_{j=0}^{m-1} g_j\, g_{m-1-j}\right)\right) \tag{68}$$

$$\text{with } \chi_m = \begin{cases} 0, & m \le 1 \\ 1, & m \ge 1 \end{cases}, \tag{69}$$

Solving the corresponding m^{th}-order deformation equations,

$$f_m(\eta) = f_m^*(\eta) + C_1 + C_2\,\eta + C_3 e^{\eta} + C_4 e^{-\eta} \tag{70}$$

$$g_m(\eta) = g_m^*(\eta) + C_5 + C_6 e^{\eta} \tag{71}$$

$$\theta_m(\eta) = \theta_m^*(\eta) + C_7 + C_8\eta \tag{72}$$

Here $f_m^*, g_m^* \; and \; \theta_m^*$ are given by are particular solutions of the corresponding mth-order equations and the constants $C_i (\, i = 1,2, \ldots ,8)$ are to be determined by the boundary conditions.

4. Result and Discussion:

This section deals with the physics of the problem. Mathematica is employed to explain effects of different parameters on velocity and heat transfer through graphs shown in Figures 1-20.

Reynolds number is proportional to the ratio of the inertial forces to viscous forces. It is evident from Figure 1 that temperature boundary layer thicknesses contracts with strengthening of Reynolds number. It is observed from Figure 2 that temperature increases with nanoparticle volume fraction. Thus nanofluids can be used efficiently as coolants in power plants. Figure 3 shows that temperature increases with Eckert number Ec. Figure 4 displays adverse effect of Prandtl number Pr on temperature profiles. It is justified as thermal conductivity of the nanofluid reduces when values of Prandtl number Pr are increased. In some of some graphs, less deviation is observed as we have considered single phase nano-fluid and also the base fluid is water (Different types of nanoparticles or base fluids can also be considered).

Figure 5 shows that velocity decreases when Reynolds number Re is increased. It is depicted from Figures 6 - 8 that magnetic field has limiting effect on flow. This is due to the Lorentz force. Figure 9 illustrates effect of nanoparticle volume fraction on fluid flow. It shows edge of nanofluids over conventional fluids as the velocity increases with decrease in nanoparticle volume fraction. Figures 10 – 12 show that velocity increases with increase in permeability parameter k. Physically it is justified as the resistance decreases. Affirmative influence of rotation parameter Kr on velocity is witnessed through Figures 12 - 13.

It is clear from Figure 14 that Skin friction increases with increase in Reynolds number. Figure 15 illustrates that skin friction can be reduced by increasing nanoparticle volume fraction. Figure 16 indicates that skin friction can also be decreased by decreasing rotation parameter Kr.

It is observed from Figures 17 – 20 that the Nusselt number has a direct provocation with nanoparticle volume fraction but it has a contradictory association with the Eckert number Ec and rotation parameter Kr.

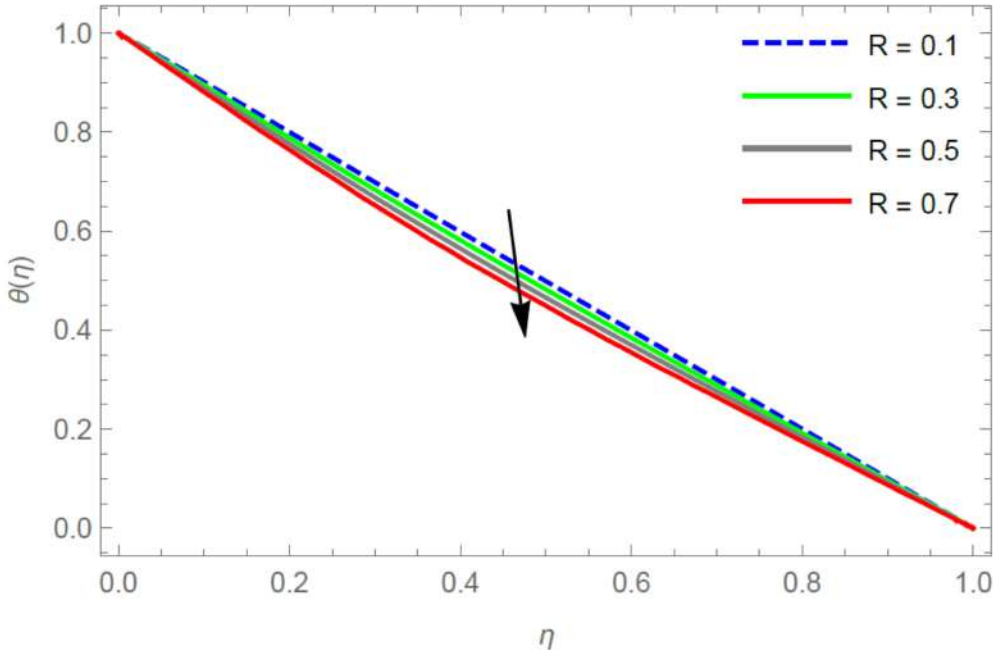

Fig 1: Temperature Profile θ for different values of η and R at M=1, Kr =1, Pr =7.2, Ec = 0.01, $\phi = 0.04$, $K = 0.2$, $Nr = 0.1$

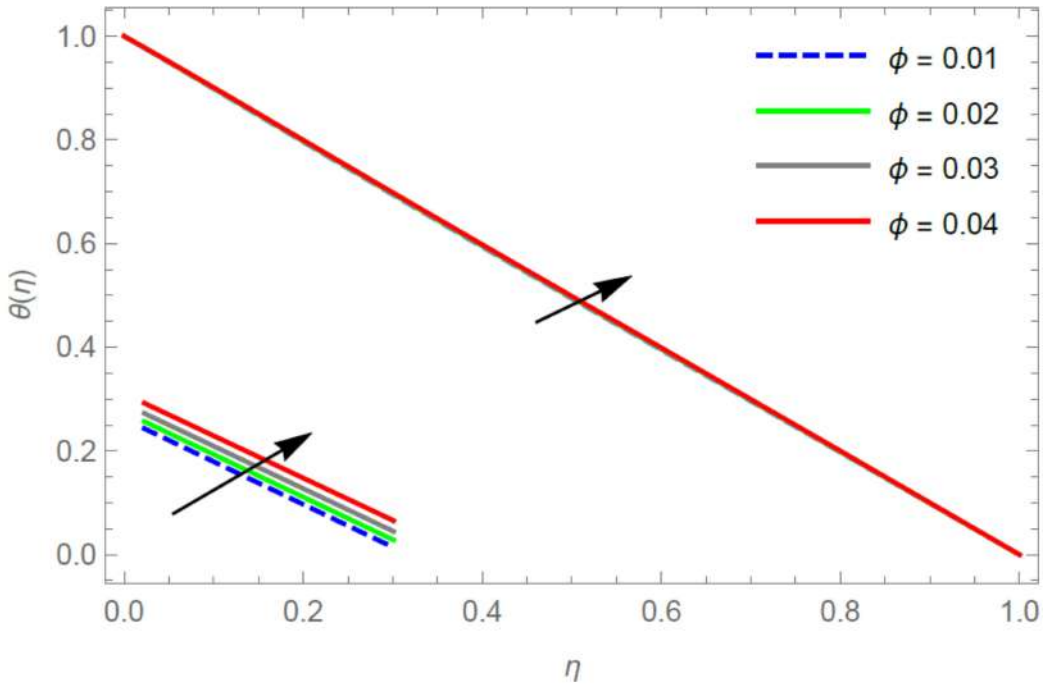

Fig 2: Temperature Profile θ for different values of η and ϕ at Kr =1, Pr =7.2, Ec = 0.01, $M = 1$, $K = 0.2$, $R = 0.1$, $Nr = 0.1$

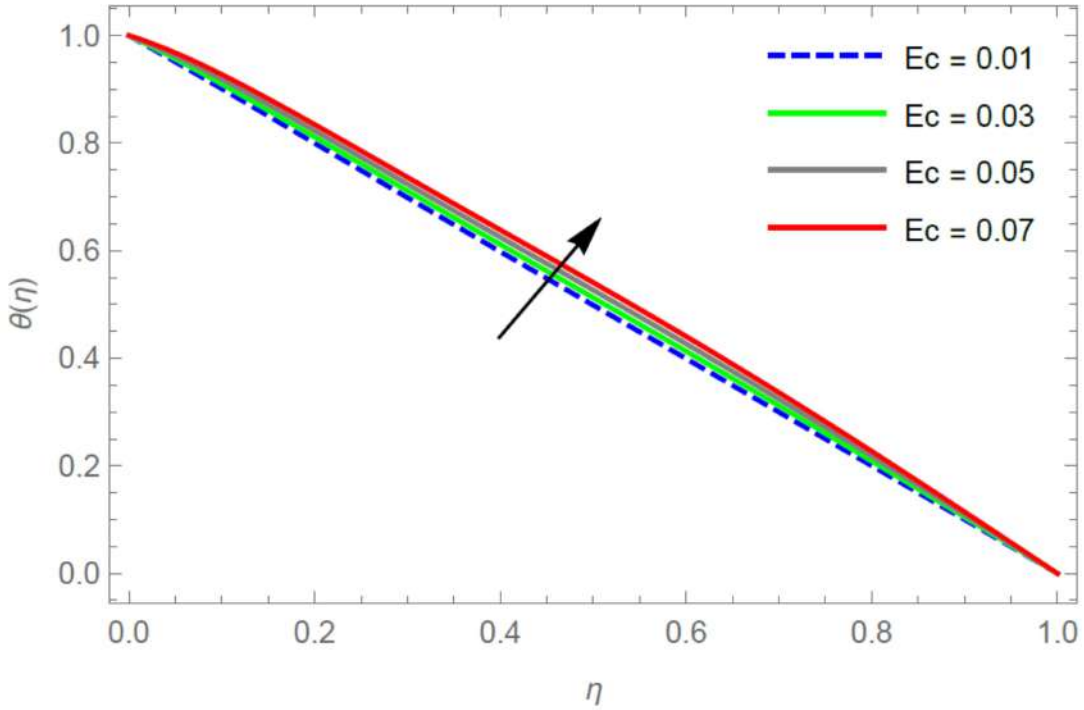

Fig 3: Temperature Profile θ for different values of η and Ec at Kr =1, Pr =7.2, $\phi = 0.04$, $M = 1$, $K = 0.2$, $R = 0.1$, $Nr = 0.1$

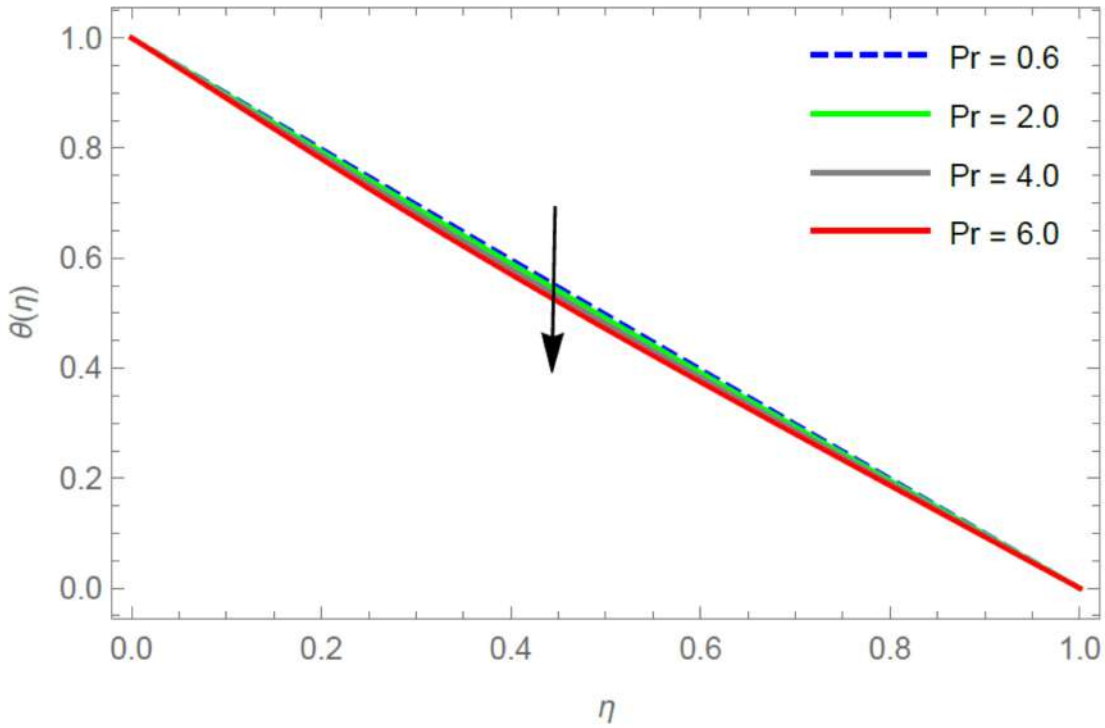

Fig 4: Temperature Profile θ for different values of η and Pr at K=0.2, Kr =1, $\phi = 0.04$, $M = 1$, $Ec = 0.01$, $R = 0.1$, $Nr = 0.1$

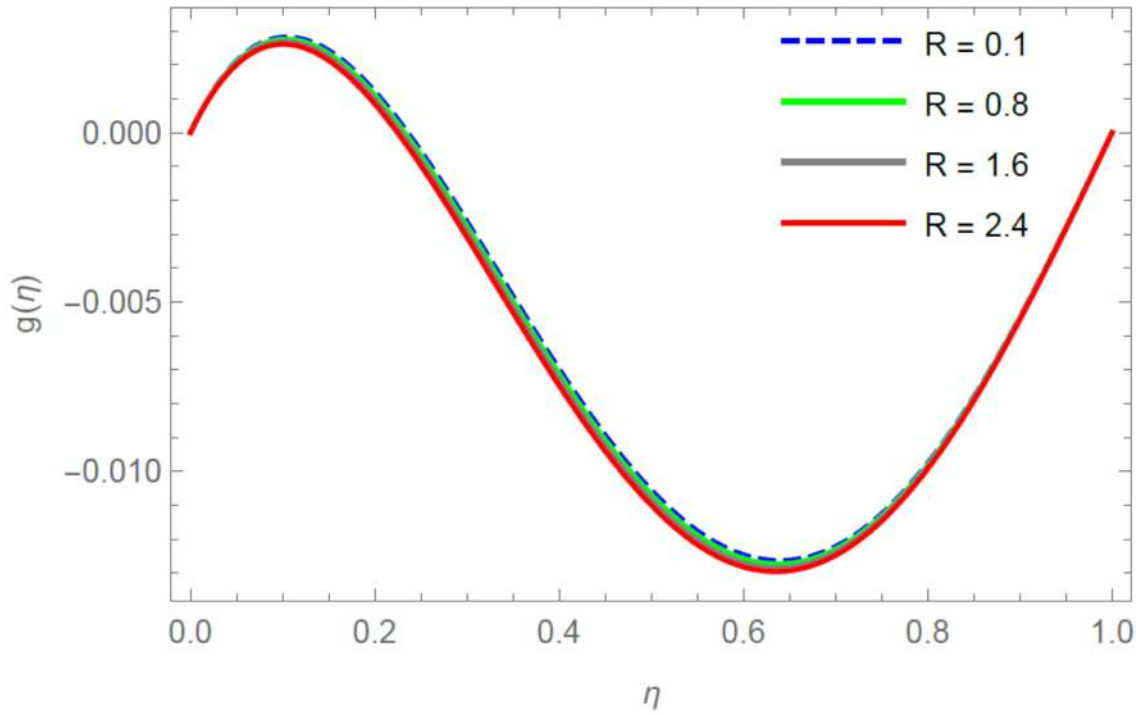

Fig 5: Velocity profile g for different values of η and R at M=1, Kr =1, Pr =7.2, Ec = 0.01, $\phi = 0.04, K = 0.2,\ Nr = 0.1$

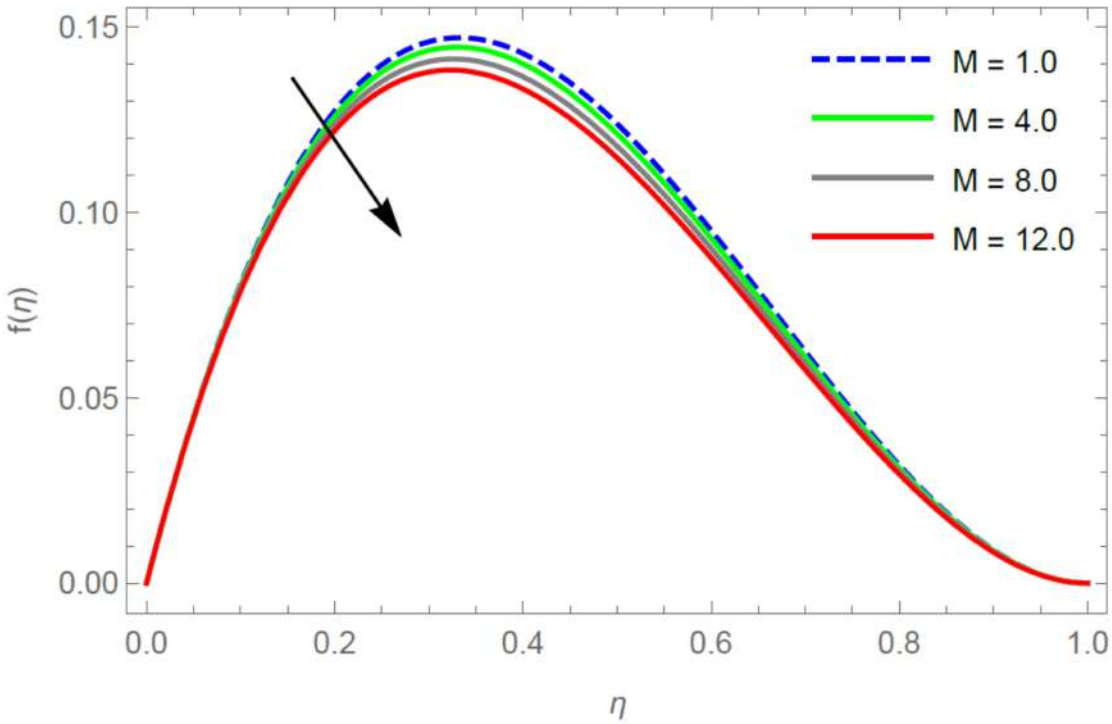

Fig 6: Velocity profile f for different values of η and M at R=0.1, Kr =1, Pr =7.2, Ec = 0.01, $\phi = 0.04, K = 0.2,\ Nr = 0.1$

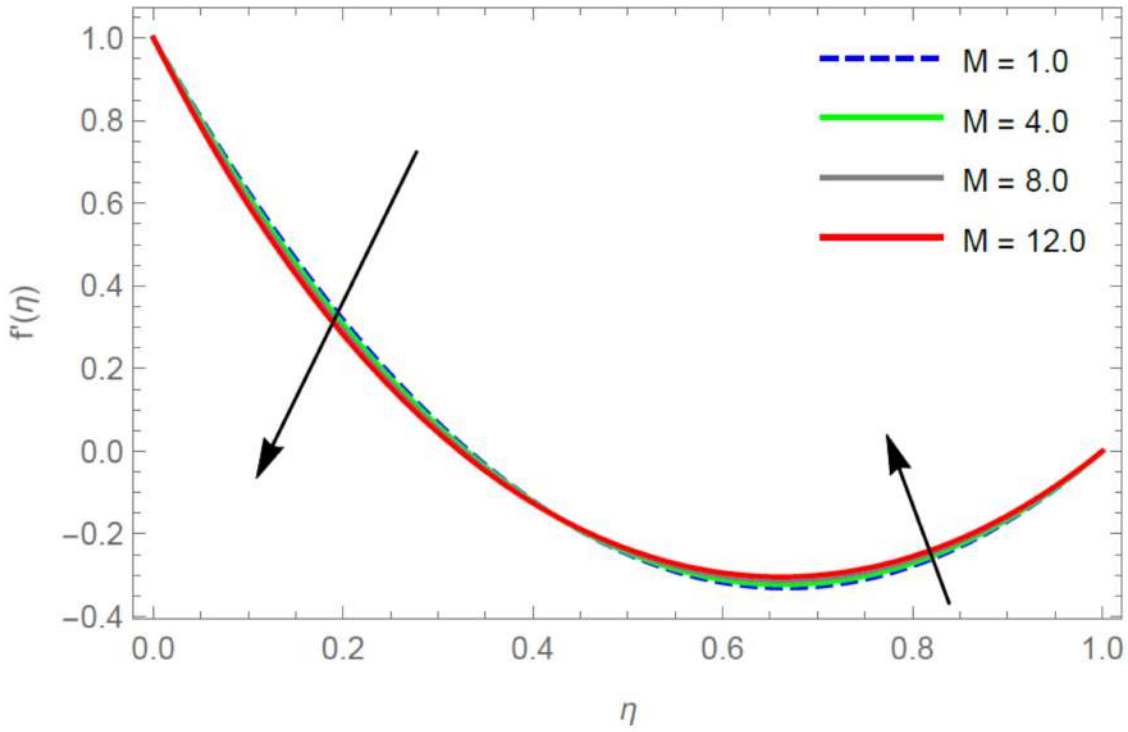

Fig 7: Velocity profile f ' for different values of η and M at R=0.1, Kr =1, Pr =7.2, Ec = 0.01, $\phi = 0.04, K = 0.2,\ Nr = 0.1$

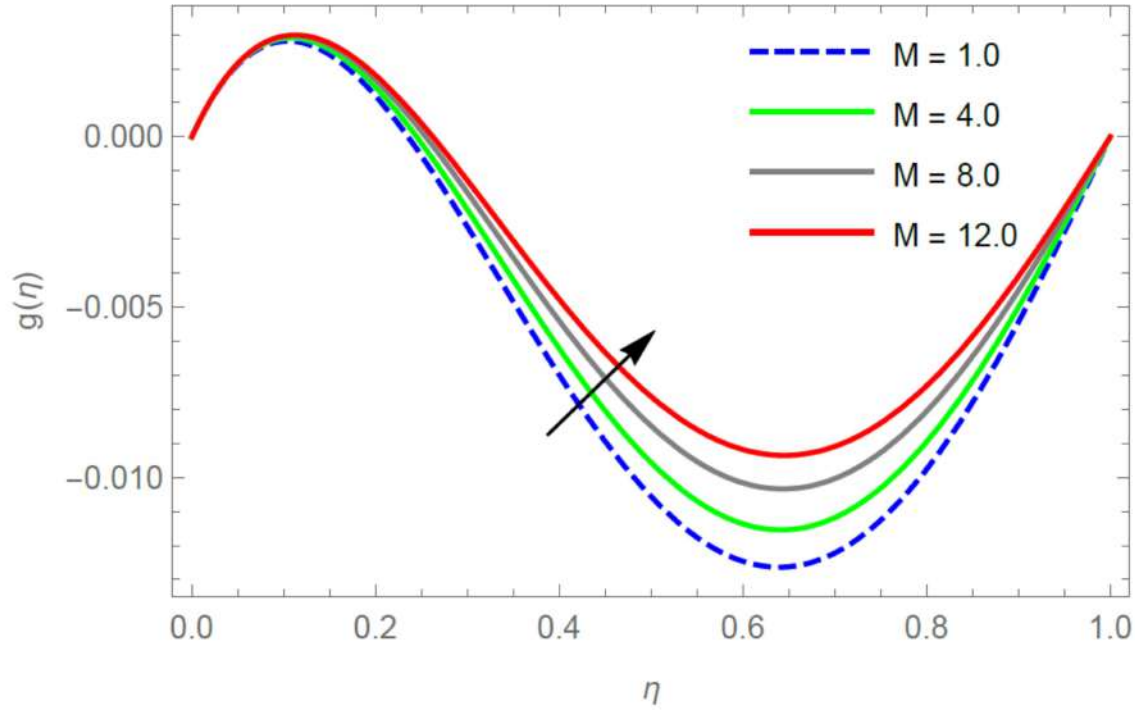

Fig 8: Velocity profile g for different values of η and M at R=0.1, Kr =1, Pr =7.2, Ec = 0.01, $\phi = 0.04, K = 0.2,\ Nr = 0.1$

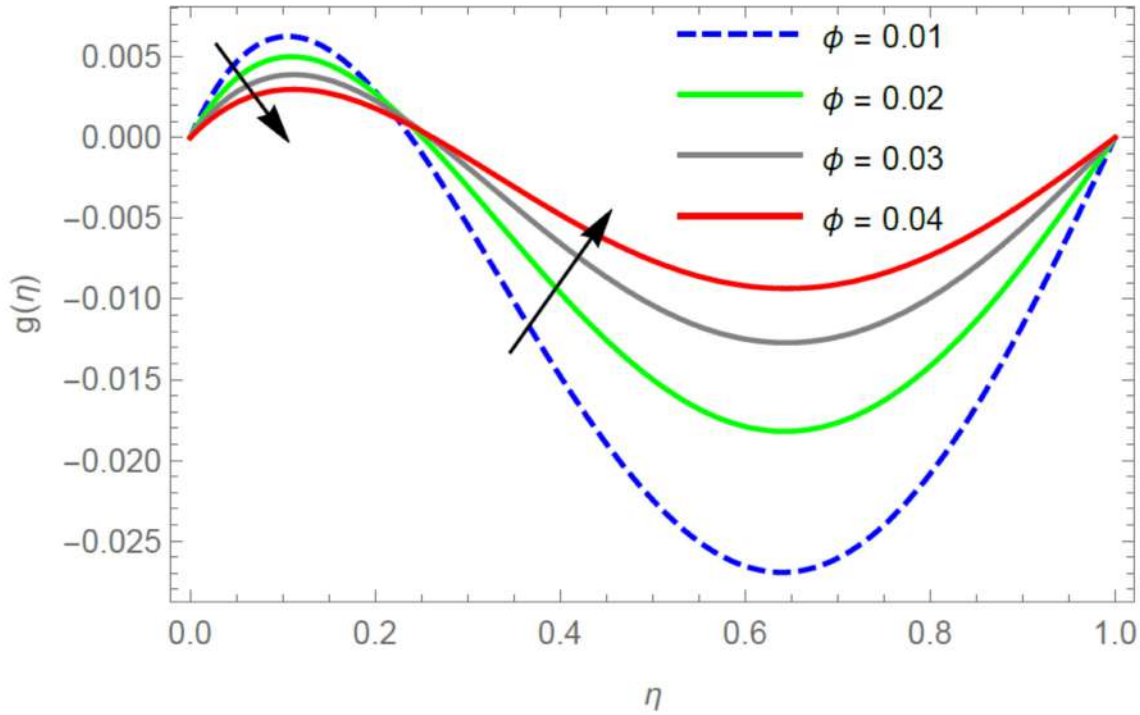

Fig 9: Velocity profile g for different values of η and ϕ at R=0.1, Kr =1, Pr =7.2, Ec = 0.01, $M = 1, K = 0.2$, $Nr = 0.1$

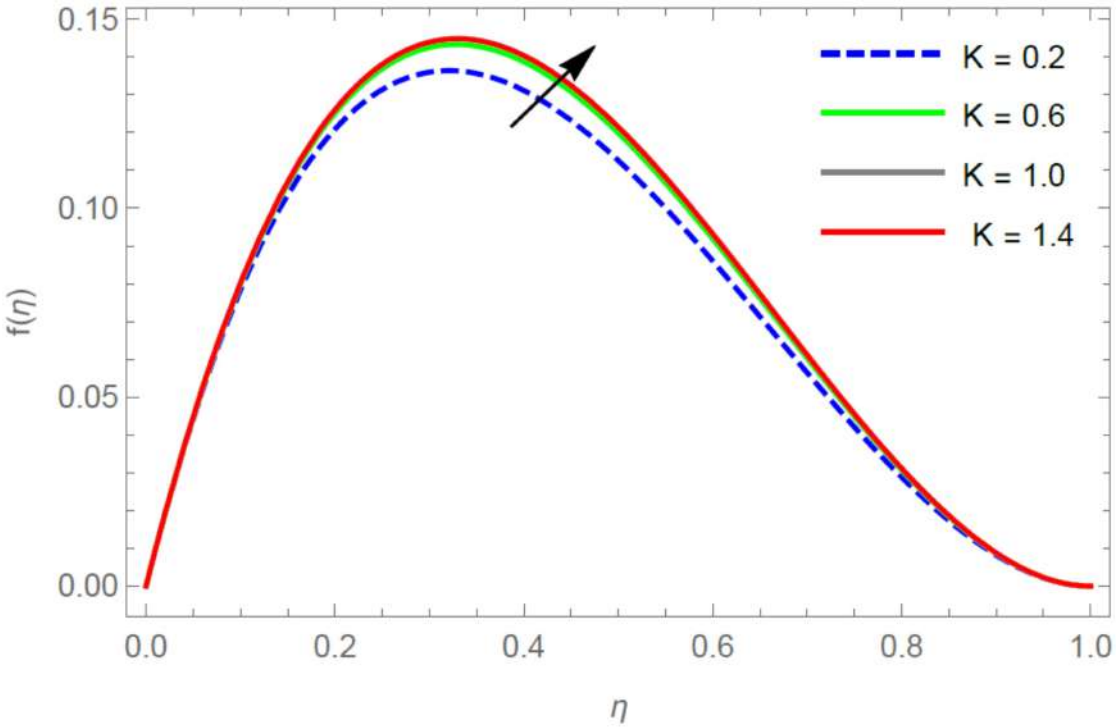

Fig 10: Velocity profile f for different values of η and K at R=0.1, Kr =1, Pr =7.2, Ec = 0.01, $M = 1, \phi = 0.04$, $Nr = 0.1$

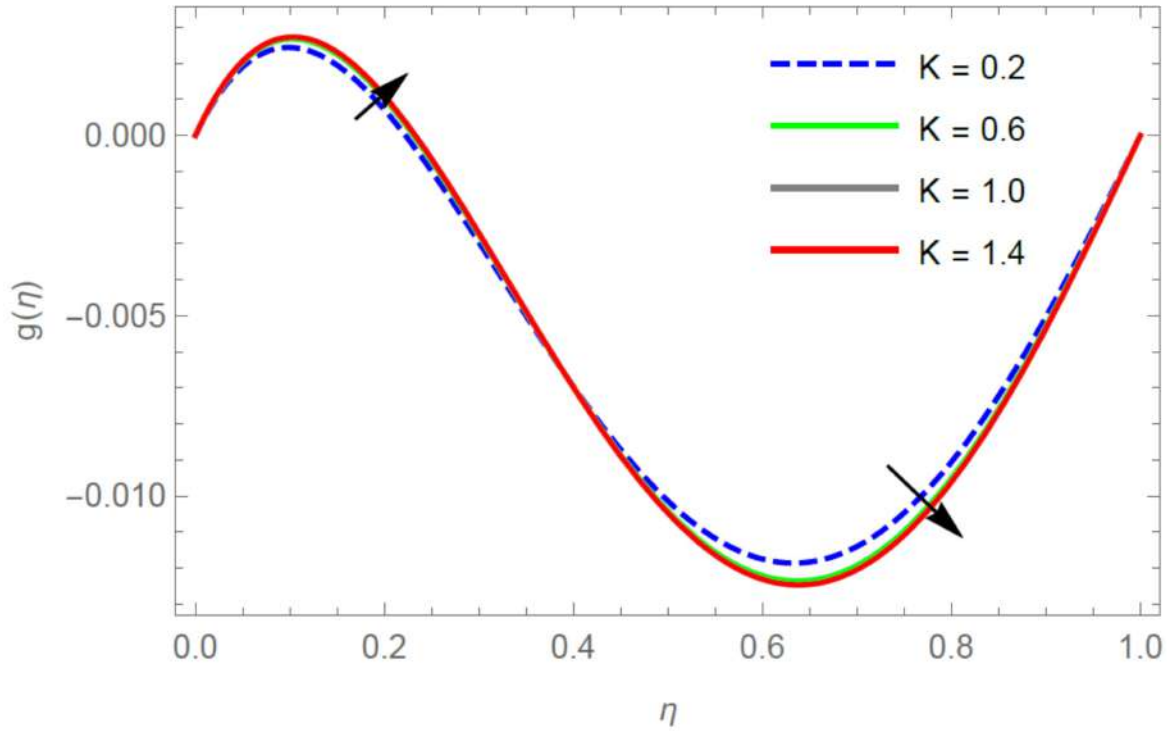

Fig 11: Velocity profile g for different values of η and K at R=0.1, Kr =1, Pr =7.2, Ec = 0.01, $M = 1,\ \phi = 0.04,\ Nr = 0.1$

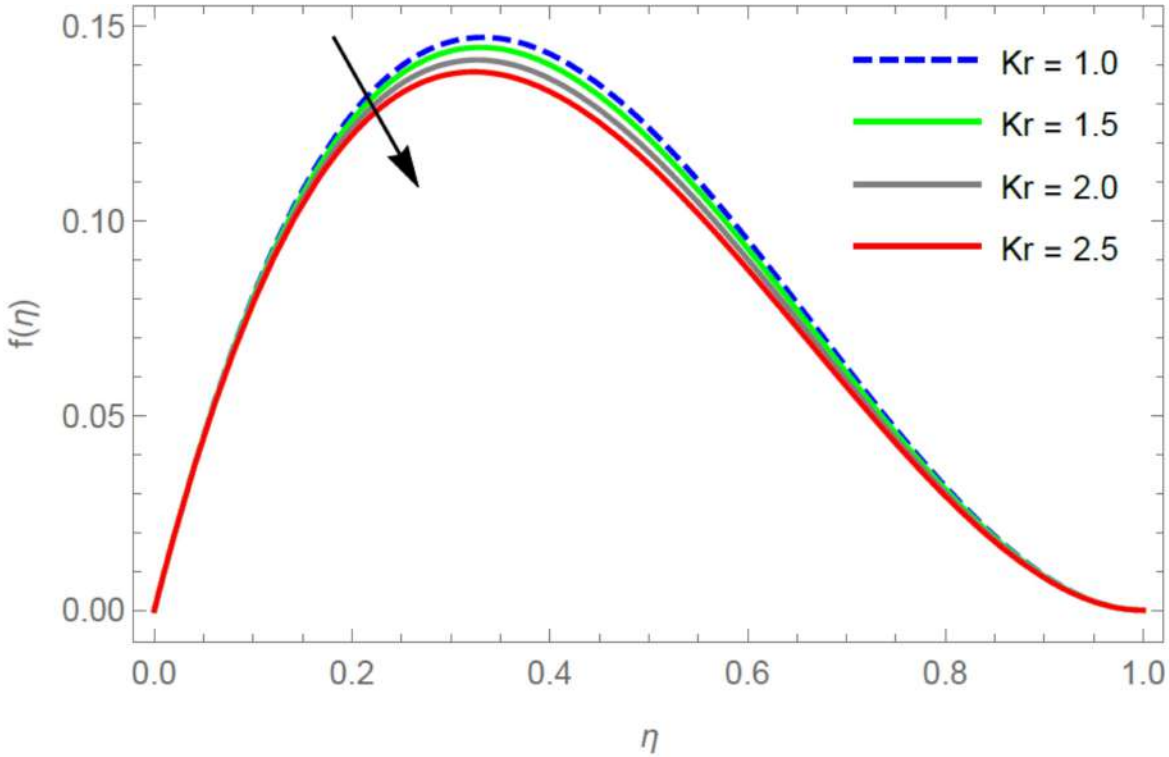

Fig 12: Velocity profile f for different values of η and Kr at R=0.1, K=0.2, Pr =7.2, Ec = 0.01, $M = 1, \phi = 0.04,\ Nr = 0.1$

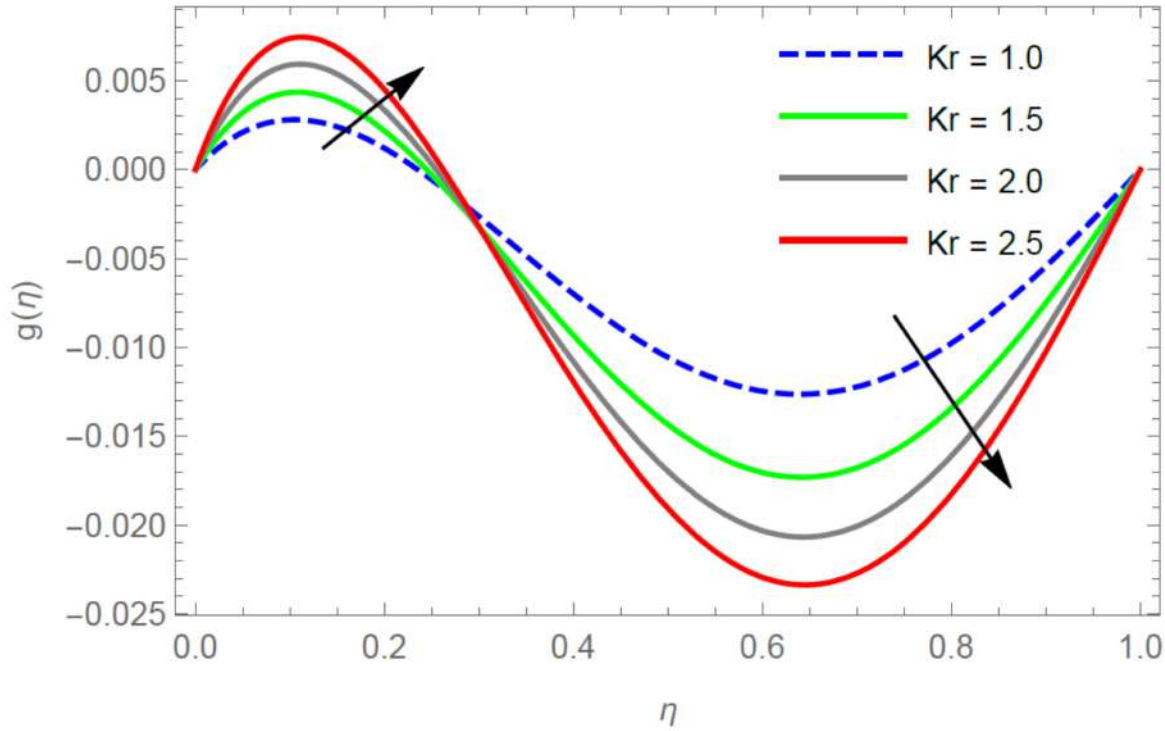

Fig 13: Velocity profile g for different values of η and Kr at R=0.1, K=0.2, Pr =7.2, Ec = 0.01, $M = 1, \phi = 0.04,\ Nr = 0.1$

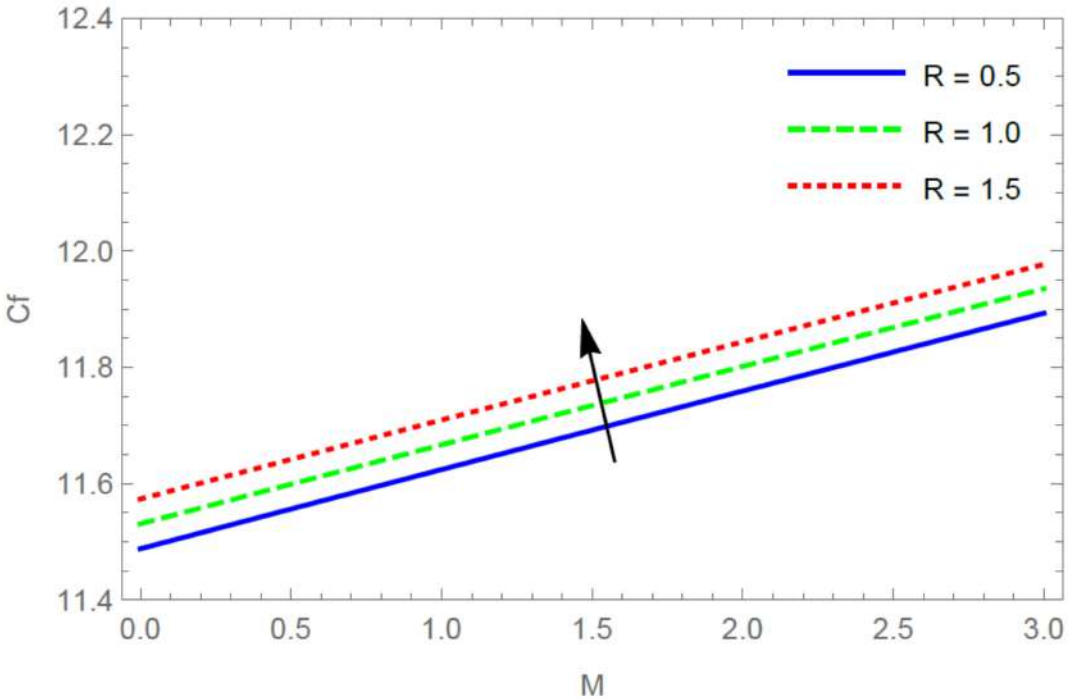

Fig 14: Effect of magnetic parameter M and R on Skin friction coefficient at Kr = 1, K=0.2, Pr =7.2, Ec = 0.01, $M = 1, \phi = 0.04,\ Nr = 0.1$

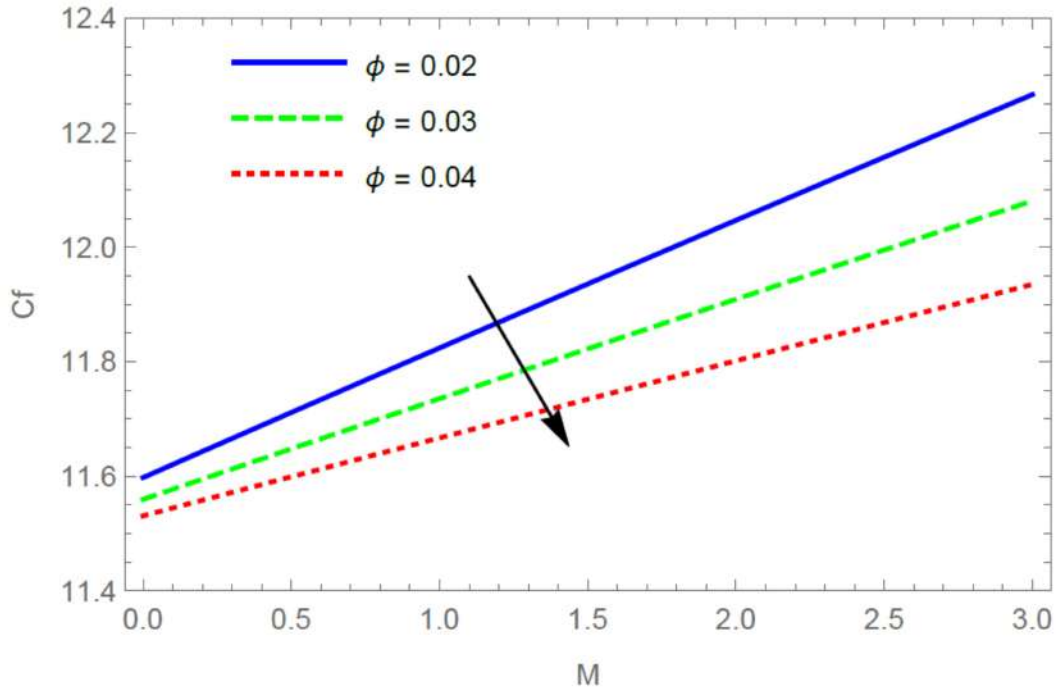

Fig 15: Effect of magnetic parameter M and ϕ on Skin friction coefficient at Kr $= 1$, K=0.2, Pr =7.2, Ec $= 0.01$, $M = 1, R = 0.1$, $Nr = 0.1$

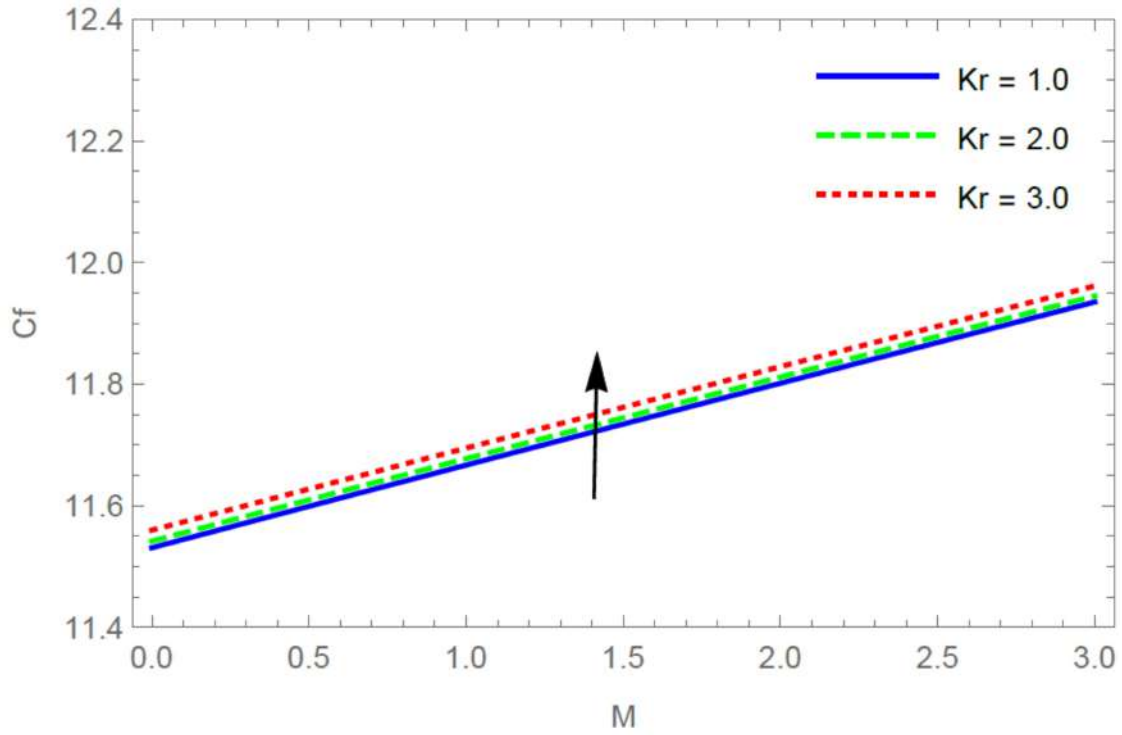

Fig 16: Effect of magnetic parameter M and Kr on Skin friction coefficient at $\phi = 0.04$, K=0.2, Pr =7.2, Ec $= 0.01$, $M = 1, R = 0.1$, $Nr = 0.1$

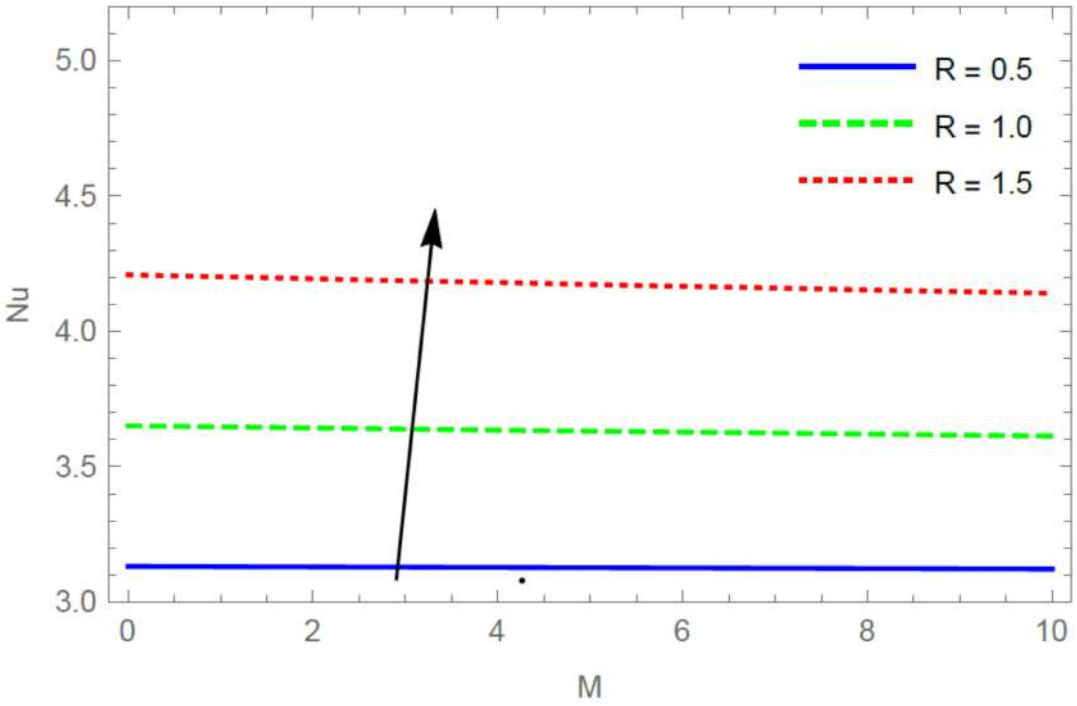

Fig 17: Effect of magnetic parameter M and R on Nusselt number at $\phi = 0.04$, K=0.2, Pr =7.2, Ec = 0.01, $M = 1$, $Kr = 1$, $Nr = 0.1$

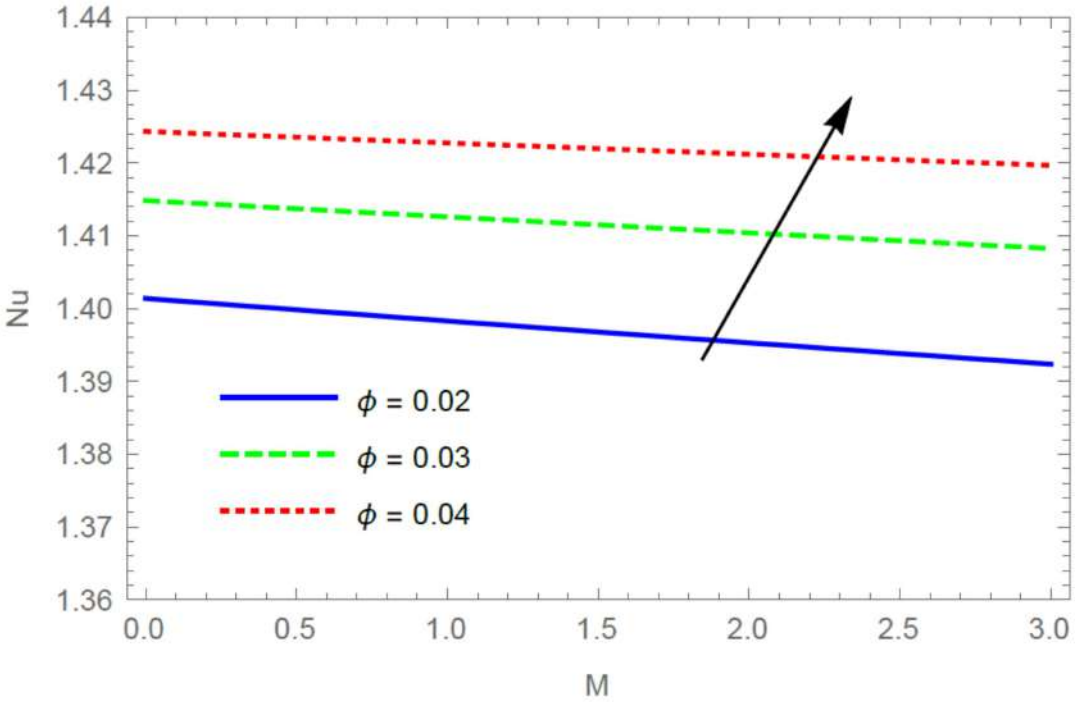

Fig 18: Effect of magnetic parameter M and ϕ on Nusselt number at $R = 0.1$, K=0.2, Pr =7.2, Ec = 0.01, $M = 1$, $Kr = 1$, $Nr = 0.1$

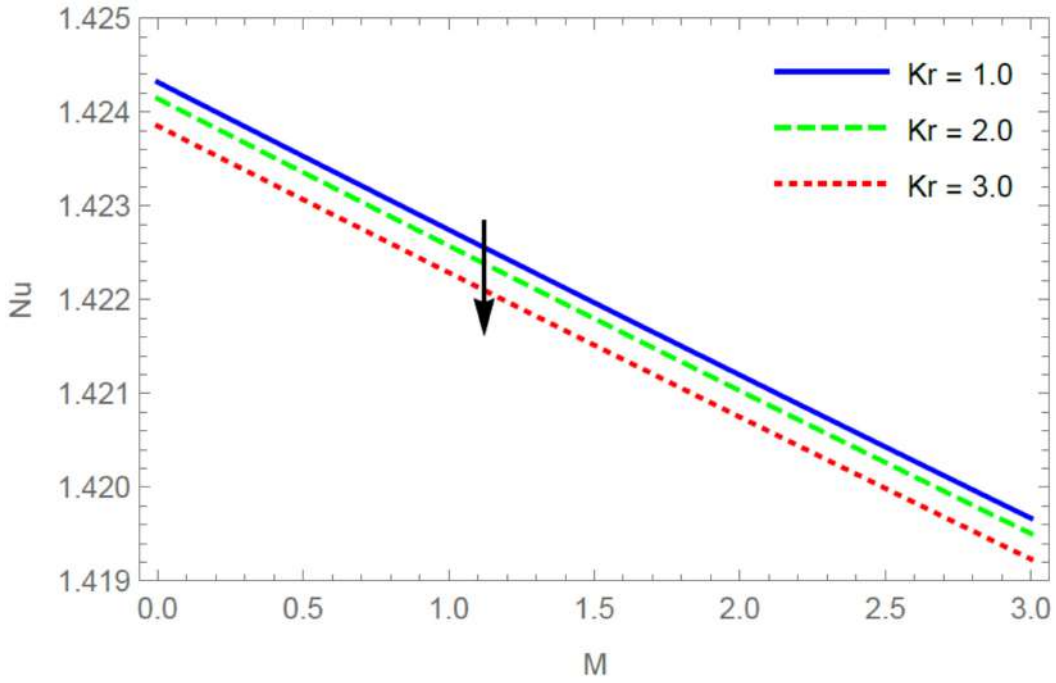

Fig 19: Effect of magnetic parameter M and Kr on Nusselt number at $R = 0.1$, K=0.2, Pr =7.2, Ec = 0.01, $M = 1$, $\phi = 0.04$, $Nr = 0.1$

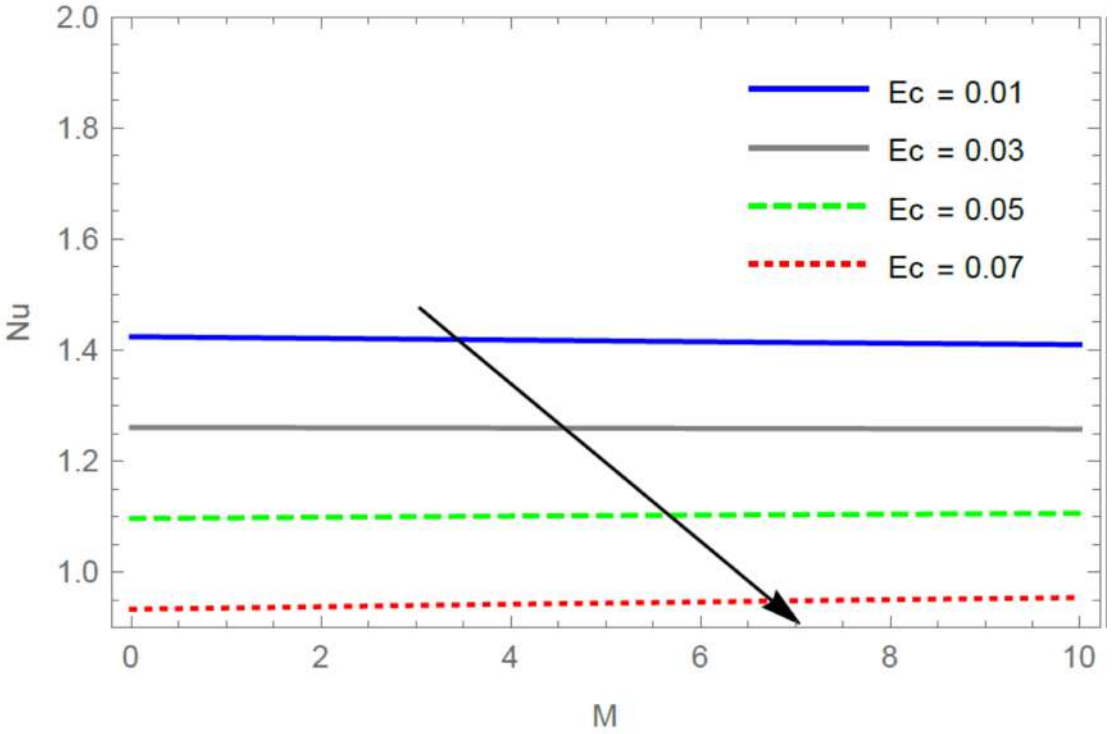

Fig 20: Effect of magnetic parameter M and Ec on Nusselt number at $R = 0.1$, K=0.2, Pr =7.2, Kr = 1, $M = 1$, $\phi = 0.04$, $Nr = 0.1$

5. References:

[1] Kataria, H. R., Mittal, A. S., (2015): Mathematical model for velocity and temperature of gravity-driven convective optically thick nanofluid flow past an oscillating vertical plate in presence of magnetic field and radiation. Journal of Nigerian Mathematical Society, 34, 303 – 317.

[2] Kataria, H. R., Mittal, A. S., (2017): Velocity, mass and temperature analysis of gravitydriven convection nanofluid flow past an oscillating vertical plate in presence of magnetic field in a porous medium, Applied Thermal Engineering, 110, 864 - 874.

[3] Kataria, H. R., Mittal, A. S., (2017): Analysis of Casson nanofluid flow in presence of magnetic field and radiation, Mathematics Today, 33(1), 99 - 120.

[4] Kataria, H. R., Patel, H. R., (2016): Effect of thermo-diffusion and parabolic motion on MHD Second grade fluid flow with ramped wall temperature and ramped surface concentration, Alexandria Engineering Journal, 10.1016/j.aej.2016.1.

[5] Kataria, H. R., Patel, H. R., (2016): Radiation and chemical reaction effects on MHD Casson fluid flow past an oscillating vertical plate embedded in porous medium, Alexandria Engineering Journal, 55, 583 - 595.

[6] Kataria, H. R., Patel, H. R., (2016): Soret and heat generation effects on MHD Casson fluid flow past an oscillating vertical plate embedded through porous medium, Alexandria Engineering Journal 55, 2125 – 2137.

[7] Kataria, H. R., Patel, H. R., (2015): Effect of magnetic field on unsteady natural convective flow of a micropolar fluid between two vertical walls. Ain Shams Engineering Journal, doi. 10.1016/j.asej.2015.08.013.

[8] Kataria, H. R., Patel, H. R., (2016): Heat and Mass Transfer in MHD Second Grade Fluid Flow with Ramped Wall Temperature through Porous Medium, Mathematics Today, 32, 67 - 83.

[9] Koo J, Kleinstreuer C (2004), Viscous dissipation effects in micro tubes and micro channels, Int. J. Heat Mass Transfer, 47, 3159–3169.

[10] Koo J, Kleinstreuer C (2005), Laminar nanofluid flow in microheat-sinks, Int. J. Heat Mass Transfer, 48, 2652–2661.

[11] Liao S J (2003), Beyond perturbation: Introduction to homotopy Analysis Method, Chapman and Hall/CRC Press, Boca Raton.

[12] Sheikholeslami, M., Kataria, H. R., Mittal, A. S., (2017): Radiation effects on heat transfer of three dimensional nanofluid flow considering thermal interfacial resistance and micro mixing in suspensions, Chinese Journal of Physics, 55, 2254 - 2272.

[13] Vajravelu, K, Kumar, B.V.R, (2004): Analytic and numerical solutions of coupled nonlinear system arising in three-dimensional rotating flow, Int. J. Non-Linear Mech. 39, 13–24.